IJITCE

ISSN 2347- 3657

International Journal of Information Technology & Computer Engineering

Email : ijitce.editor@gmail.com or editor@ijitce.com

International Journal of Information Technology & Computer Engineering

ISSN 2347–3657

Volume 7, Issue 3, 2019

NEW PHOTONIC CRYSTAL FIBER WITH A POROUS CORE BASED ON HRS FOR TERAHERTZ WAVE GUIDANCE

Dr.Sindhu R, Madhvaraja K, Firdosh Parveen S

Asst. Prof, Asst. Prof, Asst. Prof

rethisindhoo@gmail.com, madhavaraja@pdit.ac.in, firdoseks@gmail.com

Department of EEE, Proudhadevaraya Institute of Technology, Abheraj Baldota Rd, Indiranagar, Hosapete, Karnataka-583225

Abstract— An innovative PC-PCF, or Porous Core Photonic Crystal Fibre, is suggested and studied for its very low transmission loss and great birefringence. The use of high resistivity float zone silicon as the background dielectric material produces a high birefringence. X- and Y-orthogonal fundamental modes exhibit confinement losses in the order of 10-19 and 10-7, respectively, at a frequency of 1.3 THz, according to the simulation findings, and the suggested PC-PCF has an Effective Material Loss (EML) of 0.012 cm-1 and 0.0038 cm-1. The birefringence is also over 0.9. The X-polarization mode exhibits lower total losses over a broader frequency range compared to the Y-polarization mode, while retaining its strong birefringence. Additionally, we thoroughly examined the frequency-dependent changes in the core power percentage and effective modal area. Existing fabrication methods may readily produce the proposed PC-PCF because of its simple shape in both the core and cladding. Due to its strong birefringence, it might be used in terahertz medical imaging, filtration, interferometry, and sensing, among other possible uses.

***Index Terms*—birefringence, effective material loss, porous core photonic crystal fibre, terahertz**

I. INTRODUCTION

Terahertz (THz) radiation is a type of electromagnetic radiation found between microwave and infrared regions in the electromagnetic spectrum; with typical frequency span between 0.1 THz and 10 THz [1]. It is immensely popular due to its vast applications in medicine [2], communication [3], oil and gas [4], security [5], etc. Delivering broadband THz beams require efficient low loss THz waveguides. Commercially available terahertz systems are still based on open air propagation method [6], which is ineffective due to difficulties in transceiver integration and high losses due to perturbation from surrounding atmospheric conditions. Alternatively, waveguide solutions such as stainless solid wires [7], metal-coated tubes [8], and metallic-dielectric waveguides [9] have been adapted from the more matured microwave technology. However, these THz waveguide solutions are highly dissipative due to Ohmic losses [10].

Photonic Crystal Fibres (PCFs) are optical fibres that consist of subwavelength discontinuities stretching along the z-axis of their spatial extent. PCFs in the terahertz regime are categorised by their light guiding property. Whilst hollow-core PCFs (HC-PCFs) [11] operate based on photonic bandgap effect, light guidance in solid core PCFs (SC-PCFs) [10] is based on Modified Total Internal Reflection (MTIR) mechanism. Generally, SC-PCFs suffer from high material losses that arise from the characteristically lossy dielectric materials used for their constructions [10]. Porous core PCFs (PC-PCFs) [12] may be regarded as advancements of SC-PCF, in the sense that subwavelength air holes are introduced in the core region without losing their MTIR guidance property. In comparison to SC-PCFs, PC-PCFs offer lower frequency dependent transmission losses due to their great design versatility.

A number of factors need to be considered in order to design efficient PC-PCF for THz applications, with geometrical structure and type of dielectric material used among the important factors. Some commonly used materials for constructing PC-PCFs are Cyclic Olefin Polymer (COP) [13], Cyclic Olefin Copolymer (COC) [14], High-Density Polyethylene (HDPE) [14], high resistivity float zone silicon (HRS) [15], [16] etc.

Efforts have been made to increase the birefringence of COC, COP and HRS-based PC-PCFs while simultaneously maintaining low transmission losses [17]-[25]. Ahmed *et al*. [17] has proposed COC-based birefringent PC-PCF with birefringence of 0.012 and effective material loss (EML) of 0.068 cm^{-1}, however, core power fraction has not investigated [17]. Slight improvement in birefringence of 0.035 has been achieved with the proposal of triple air hole in the core in reference [18]. However, the fibre exhibits very high EML of 0.4 cm^{-1}. Another previously reported COC-based PC-PCF [19] exhibits a birefringence of 0.051, EML of 0.07 cm^{-1} and power fraction of 38%. However, the structure was composed of too many elliptical air holes in its core, which may complicate fabrication process. COP-[20] and COC-based [21] PC-PCFs have been proposed showing birefringence within 0.05 to 0.079, EML above 0.05 cm^{-1} and maximum power fraction of 45%. For COC-based PC-PCF, highest birefringence of 0.086 has been reported by Islam *et al*. [22], [23].

International Journal of Information Technology & Computer Engineering
ISSN 2347–3657
Volume 7, Issue 3, 2019

Amongst dielectric materials with high transparency in THz frequencies, HRS, with absorption coefficient below 0.025 cm^{-1} from 1.1 THz to 2 THz and below 0.01 cm^{-1} between 0.2 THz and 1.1 THz, is the most transparent. HRS also has a near constant refractive index profile of 3.417 from 0.1 THz to 4.5 THz. Additionally, HRS has negligible intrinsic group velocity dispersion. These excellent properties lead to the development of HRS-based PCFs with length of up to 100 cm for propagation of terahertz radiation [16]. Using HRS and an epsilon-near-zero (ENZ) material, Yang *et al.* [24] has achieved higher birefringence of 0.28 with loss below 0.01 cm^{-1}. An even higher birefringence of 0.82 has been achieved by the same research group [25], but by using HRS based PC-PCF consisting of 8 triangular slots in the core.

II. Geometry of the Proposed Design

Fig. 1 shows the cross-section geometry of the proposed PC-PCF. The cladding is made up of eighty-four circular air holes with diameter d. Four elliptical air holes e_1, e_2, e_3 and e_4 are introduced in the core, all having the same minor axis b, with major axis a_1 for e_1 and e_4, and major axis a_2 for e_2 and e_3 The elliptical air holes e_1 and e_2 as well as e_3 and e_4, are separated by Λ_1, with distance between the identical pair defined as Λ_2. Porosity is defined as the ratio of the cumulative area of all four elliptical air holes to the total core cross-section area, with core diameter given by $2(\Lambda - d/2)$. High porosity of 0.85 is maintained to destroy the geometrical symmetry thus achieving high birefringence. Beyond the computational domain, anisotropic perfectly matched layer (PML) is assigned to absorb incident radiation and prevent it from reflecting back to the fibre.

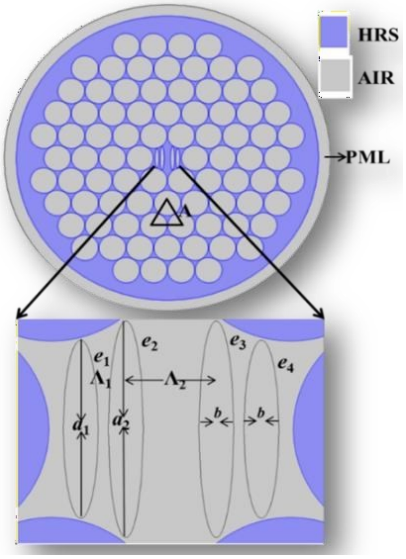

Fig. 1. Proposed PC-PCF with triangular lattice arrangement in the cladding and four elliptical air holes in the core, spanning the spatial extent of the core region.

III. Analysis Method

To investigate the characteristics of the proposed PC-PCF, full vectorial finite element method (FV-FEM) based COMSOL multiphysics software is utilized. In FV-FEM, the geometrical structure shown in Fig. 1 is discretized into smaller elements using the meshing process. These nodes are solved individually to attain a more accurate result. Additionally, fine mesh type is used to produce 384 vertex elements, 7267 edge elements, and 80,300 triangular elements. Average element quality of about 0.9299 is obtained from the mesh analysis.

IV. Simulation Results

Phase velocity or refractive index of any fundamental mode is called effective refractive index. Two orthogonal fundamental modes are found due to the induced geometrical asymmetry. The difference between these two orthogonal modes causes birefringence B which is expressed as [26]

$$B = \mathrm{Re}\left|n_{\mathrm{eff}}^{x} - n_{\mathrm{eff}}^{y}\right| \quad (1)$$

where $\mathrm{Re}(n_{\mathrm{eff}}^{x})$ and $\mathrm{Re}(n_{\mathrm{eff}}^{y})$ are the real part of the effective refractive indexes of the two orthogonal fundamental modes.

Dependence of birefringence on frequency is shown in Fig. 2. The proposed PC-PCF exhibits ultra-high birefringence of 0.4 to 0.92 within 0.7 THz to 1.5 THz range (0.8 THz band) at 100 µm pitch. It can be seen that birefringence escalates with increasing frequency. The escalation is due to the increased difference in refractive index between the orthogonal modes. It is also observed that birefringence gradually reduces after certain frequency; due to increased scattering and EML of the fibre which consequently reduces incremental rate of the refractive index difference between the two orthogonal modes. Highest birefringence is achieved at frequency 1.3 THz with Λ=100 µm which forms the basis of analysis for the rest of the paper.

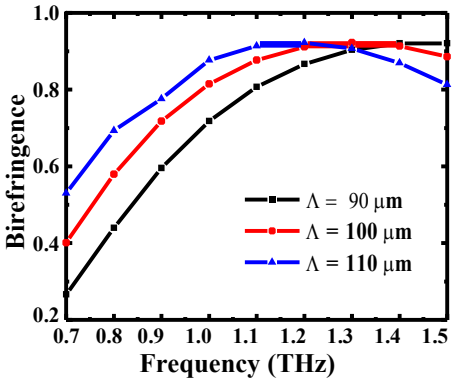

Fig. 2. Birefringence of the proposed PC-PCF in relation to frequency.

Effective material loss, α_{eff} is an important property of PC-PCFs, which is fundamentally influenced by the intrinsic absorption coefficient of HRS and may be reduced by accessing high porosity values in the core. EML per unit length in centimetres, is quantified by using the following equation [25]:

$$\alpha_{\mathrm{eff}} = \frac{(\varepsilon_0/\mu_0)^{\frac{1}{2}} \int n_{\mathrm{mat}} \alpha_{\mathrm{mat}} |E|^2 \, dA}{\int_{\mathrm{All}} S_z dA} \quad (2)$$

International Journal of Information Technology & Computer Engineering
ISSN 2347–3657
Volume 7, Issue 3, 2019

where ε_0 and μ_0 are the permittivity and permeability of free space, α_{mat} is absorption coefficient of the host dielectric, n_{mat} is the refractive index of HRS, E is electric field intensity and S_z is the z component of the Poynting vector.

Fig. 3 captures the direct dependence of EML on frequency, i.e. EML increases as frequency increases. This occurs because of the increasing light-matter interaction at higher frequency [27]. Moreover, EML of the proposed fibre is extremely low for both polarisation modes, where within 0.7 THz to 1.5 THz frequency range, EML is less than 0.015 cm^{-1} for the X-polarisation (XP) mode and below 0.006 cm^{-1} for the Y-polarisation (YP) mode. EML of the X- and Y-polarisation modes at 1.3 THz operating frequency are 0.012 cm^{-1} and 0.0038 cm^{-1}, representing 20% and 75% reduction from HRS absorption coefficient respectively. It can be observed that EML of the Y-polarisation mode is much lower than that of the X-polarisation mode. This is due to the fact that much more THz light is incident on the solid dielectric in the X-polarisation mode, as can be seen from the electric field distribution displayed in Fig. 4.

Confinement loss is an important property that provides information on the localization of light in the core region. It is calculated by using imaginary part of the complex effective refractive index and measured per unit length [25]:

$$L_C = \frac{4\pi f}{c} \times \mathrm{Im}\left[n_{\mathrm{eff}}\right] \qquad (3)$$

where f is the operating frequency in THz, c is the velocity of light in free space, Im(n_{eff}) is the imaginary part of the effective refractive index derived by solving Maxwell's equations.

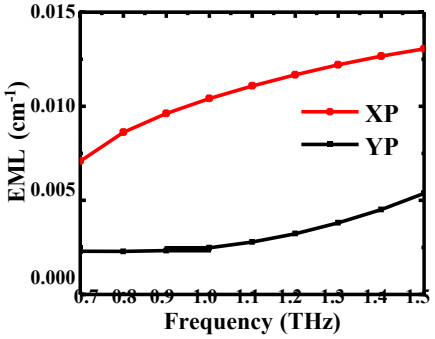

Fig. 3. EML of the proposed PC-PCF for X- and Y-polarisation modes in relation to frequency.

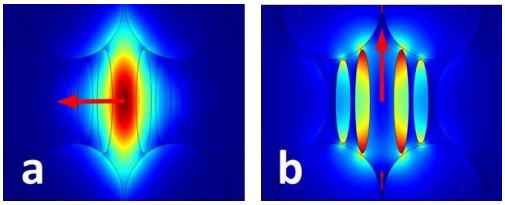

Fig. 4. Electric field distribution of proposed HRS PC-PCF at Λ = 100 µm and 1.3 THz source frequency, with red arrows indicating direction of propagation for (a) X-polarisation and (b) Y-polarisation modes.

Fig. 5 shows the dependence of confinement loss on frequency, with confinement loss reducing with an increase in frequency. This is due to the fact that refractive index of the core is directly proportional to frequency whilst that of the cladding remains fixed. This boosts core-cladding refractive index contrast and consequently improves localisation of light in the porous core. Furthermore, it can be seen from the electric field distributions that THz light is actually highly confined to the core region of the fibre. Confinement loss of the proposed fibre is 1.18×10 $^{-19}$ cm^{-1} in the X-polarisation mode and 7.9×10 $^{-7}$ cm^{-1} in the Y-polarisation mode, at frequency 1.3 THz.

Total loss is a combination of EML and confinement loss and it represents holistic view of the proposed fibre's transmission loss. Fig. 6 shows total loss of the proposed PC-PCF. It can be seen that the X-polarisation mode's total loss is extremely flattened within the entire examined frequency range while the Y-polarisation mode's total loss is only extremely low and flattened within 1 THz to 1.5 THz.

It is desired for a guided mode to be propagated through the elliptical air holes as THz light has negligible absorption in dry air. This amount of useful light is called power fraction (PF), η' and can be calculated using the following expression [28], [29]:

$$\eta' = \frac{\int_x S_z dA}{\int_{\mathrm{all}} S_z dA} \qquad (4)$$

where region x corresponds to the elliptical air holes of interest.

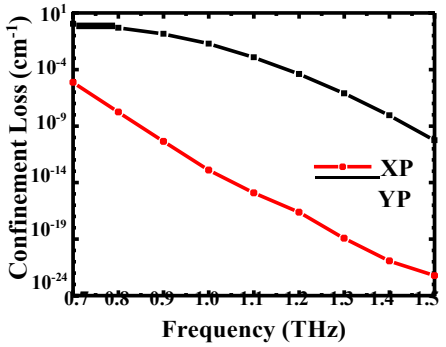

Fig. 5. Confinement loss of the proposed PC-PCF for X and Y polarisation modes in relation to frequency.

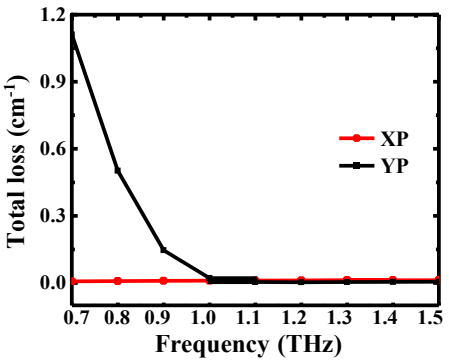

Fig. 6. Total loss of the proposed PC-PCF for X and Y polarisation modes in relation to frequency.

Fig. 7 depicts power fraction in the elliptical air holes as a function of frequency for the proposed PC-PCF. X-

International Journal of Information Technology & Computer Engineering
ISSN 2347–3657
Volume 7, Issue 3, 2019

polarisation power fraction is observed to be lower than Y-polarisation power fraction at 1.3 THz operating frequency; due to the fact that higher amount of THz light is propagated through elliptical air holes on the Y-polarisation. At 1.3 THz, power fractions of the proposed PC-PCF in the X- and Y-polarisation modes are 27% and 46%, respectively. The rest of the power is distributed across HRS substrate and cladding air holes.

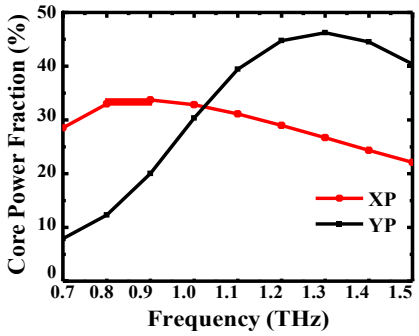

Fig. 7. Core power fraction of the proposed PC-PCF for X- and Y-polarisation modes in relation to frequency.

Effective mode area A_{eff} is a quantitative measure of the total area that the fundamental mode of the fibre covers in transverse dimensions. It is quantified by the following expression [28]:

$$A_{\text{eff}} = \frac{\left[\int I(r)\, rdr\right]^2}{\int I^2(r) rdr} \quad (5)$$

where $I(r)$ represents intensity of THz light incident on the proposed PC-PCF and r represents radial distance.

Fig. 8 presents the effective area for both orthogonal modes. It is noticeable that area covered by the fundamental mode decreases with increase in frequency, as more light is confined in the core region as frequency increases. Simulated effective area for the X- and Y-polarization modes are 3.9×10^{3} μm^2 and 4.83×10^{3} μm^2 for 1.3 THz frequency.

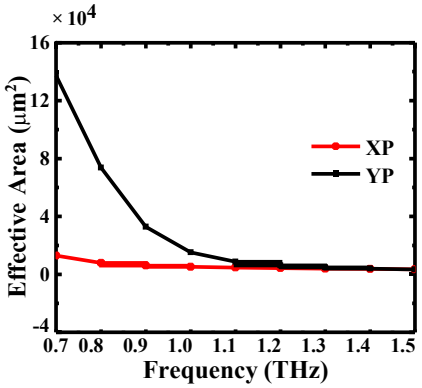

Fig. 8. Effective area of the proposed PC-PCF for X- and Y-polarisation modes in relation to frequency.

Table I shows comparison between the proposed PC-PCF and other birefringent PC-PCFs. It can be seen that HRS-based PC-PCFs yield higher birefringence than COC and COP based PC-PCFs, due to higher material refractive index of HRS. Comparing against HRS-based PC-PCFs, the proposed PC-PCF produces even higher birefringence than existing HRS-based PC-PCFs. EML and L_c are also extremely low, with large amount of useful power propagated through the elliptical air holes.

TABLE I. COMPARISON BETWEEN PROPOSED PC-PCF AND OTHER BIREFRINGENT FIBRES

Ref.	Mat.	B	EML (cm^{-1})	L_c (cm^{-1})	PF (%)
[20]	COP	0.063	0.06	10^{-10}	45
[21]	COC	0.075	0.08	10^{2}	45
[22]	COC	0.086	0.05	10^{-9}	-
[23]	COC	0.086	0.065	10^{-9}	-
[24]	HRS	0.28	0.01	-	-
[25]	HRS	0.82	0.004	0.004	-
Proposed	HRS XP		0.01	10^{-19}	27
PC-PCF	HRS YP	0.923	0.003	10^{-7}	46

V. CONCLUSION

A HRS-based birefringent PC-PCF with low transmission loss has been designed, simulated and studied for terahertz wave propagation. Modal characteristics of the proposed fibre are established using full vectorial finite element method with meshing discretization. To achieve ultra-high birefringence, symmetry between the X and Y polarization modes has been destroyed by introducing elliptical air holes in the core.

The proposed PC-PCF exhibits an extremely high birefringence of 0.923 and an extremely low EML of 0.012 cm^{-1} and 0.0038 cm^{-1} for X- and Y-orthogonal modes, respectively, at frequency 1.3 THz. Negligibly low confinement losses, in the order of 10^{-19} cm^{-1} and 10^{-7} cm^{-1} for the X- and Y-polarization modes have also been obtained, also at frequency 1.3 THz. In addition, about 46% of useful power is transmitted through its quad-elliptical air holes. PC-PCFs with such high birefringence and low loss property are suitable for polarization demanding THz applications such as sensing, security, THz medical imaging, etc. It is anticipated that existing fabrication technologies can be employed to implement this PC-PCF for integration into industrial THz devices.

REFERENCES

[1] S. S. Dhillon, M. S. Vitiello, E. H. Linfield, A. G. Davies, M. C. Hoffmann, J. Booske, *et al*., "The 2017 terahertz science and technology roadmap," *Journal of Physics D*, vol. 50, no. 4, pp. 1-49, 2017.

[2] C. Yu, S. Fan, Y. Sun, and E. Pickwell-Macpherson, "The potential of terahertz imaging for cancer diagnosis: A review of investigations to date," *Quantitative Imaging in Medicine and Surgery*, vol. 2, no. 1, pp. 33–45, 2012.

[3] A. Y. Nikitin, "Telecom meets terahertz," *Nature Photonics*, vol. 12, no. 1, pp. 3–4, 2018.

[4] H. Zhan, S. Wu, R. Bao, L. Ge, and K. Zhao, "Qualitative identification of crude oils from different oil fields using terahertz Time-Domain spectroscopy," *Fuel*, vol. 143, no. 23, pp. 189–193, 2015.

[5] M. A. Startsev and A. Y. Elezzabi, "Terahertz frequency continuous-wave spectroscopy and imaging of explosive substances," *ISRN Optics*, vol. 2013, pp. 1–8, January 2013.

[6] D. O. Otuya, K. Kasai, M. Yoshida, T. Hirooka, and M. A. Nakazawa, "Single-channel 192 tbit/s, 64 qam coherent optical pulse transmission over 150 km using frequency-domain

ISSN 2347–3657

Volume 7, Issue 3, 2019

equalization," *Optics Express*, vol. 21, pp. 22808-22816, Sept. 2013.

[7] W. Kanglin and M. M. Daniel, "Metal wires for terahertz wave guiding," *Letters to Nature*, vol. 432, pp. 376-379, November 2003.

[8] R. W. McGowan, G. Gallot, and D. Grischkowsky, "Propagation of ultra-wideband short pulses of terahertz radiation through submillimeter-diameter circular waveguides," *Optics Letters*, vol. 24, pp. 1431-1433, June 1999.

[9] M. Wächter, M. Nagel , and H. Kurz, "Frequency-dependent characterization of thz sommerfeld wave propagation on Single-Wires," *Optics Express*, vol. 13, pp. 10815-10822, December 2005.

[10] S. Atakaramians, S. Afshar, T. M. Monro, and D. Abbott, "Terahertz dielectric waveguides," *Advances in Optics and Photonics*, vol. 5, no. 2, pp. 169–215, July 2013.

[11] C. S. Ponseca, R. Pobre, E. Estacio, N. Sarukura, A. Argyros, M. C. J. Large, and M. A. van Eijkelenborg, "Transmission of terahertz radiation using a microstructured polymer optical fiber," *Optics Letters*, vol. 33, no. 9, pp. 902-904, May 2008.

[12] A. Hassani, A. Dupuis, and M. Skorobogatiy, "Polymer fibers for low-loss terahertz guiding," *Optics Express*, vol. 16, pp. 6340–6351, April 2008.

[13] J. Anthony, R. Leonhardt, A. Argyros, and M. C. J. Large, "Characterization of a microstructured zeonex terahertz fiber," *Journal of Optical Society of America B*, vol. 28, pp. 1013-1018, April 2011.

[14] P. D. Cunningham, N. N. Valdes, F. A. Vallejo, L. M. Hayden, B. Polishak, X. H. Zhou, *et al.*, "Broadband terahertz characterization of the refractive index and absorption of some important polymeric and organic electro-optic materials," *Journal Applied Physics*, vol. 109, no. 4, pp. 043505-043505-5, February 2011.

[15] B. Kuyken, A. Pagies, M. Vanwolleghem, N. D. Yarekha, J. F. Lampin, and G. Roelkens, "Low loss silicon waveguides for the terahertz spectral region," presented at the 40th International Conference on Infrared, Millimeter, and Terahertz Waves, 2015.

[16] J. Dai, J. Zhang, W. Zhang, and D. Grischkowsky, "Terahertz time-domain spectroscopy characterization of the Far-Infrared absorption and index of refraction of high-resistivity, float-zone silicon," *Journal of Optical Society of America B*. vol. 21, 7, pp. 1379-1386, July 2004.

[17] K. Ahmed, S. Chowdhury, B. K. Paul, S. Islam, M. Sen, S. I. Islam, and M. S. Asaduzzaman, "Ultrahigh birefringence, ultralow material loss porous core single-mode fiber for terahertz wave guidance," *Applied Optics*, vol. 56, pp. 3477-3483, April 2017.

[18] Z. Wu, X. Zhou, H. Xia, Z. Shi, J. Huang, X. Jiang, and W. Wu, "Low-loss polarization-maintaining thz photonic crystal fiber with a triple-hole core," *Applied Optics*, vol. 56, pp. 2288-2293, March 2017.

[19] M. A. Habib and M. S. Anower, "Design and numerical analysis of highly birefringent single modefiber in THz regime," *Opt. Fiber Technol.*, vol. 47, pp. 197–203, January 2019.

[20] M. S. Islam, J. Sultana, A. Dinovitser, M. Faisal, M. R. Islam, B. W. H. Ng, and D. Abbott, "Zeonex-based asymmetrical terahertz photonic crystal fiber for multichannel communication and polarization maintaining applications," *Applied Optics*, vol. 57, pp. 666-672, January 2018.

[21] R. Islam, M. Habib, S. Hasanuzzaman, G. K. M. Ahmad, R. Rana, and S. F. Kaijage, "Extremely high-birefringent asymmetric slotted-core photonic crystal fiber in thz regime," *IEEE Photonics Technology Letters*, vol. 27, pp. 2222–2225, November 2015.

[22] J. Sultana, M. S. Islam, M. Faisal, M. R. Islam, B. W. H. Ng, H. E-. Heidepriem, and D. Abbott, "Highly birefringent elliptical core photonic crystal fiber for terahertz application," *Optics Communication*, vol. 407, pp. 92–96, January 2018.

[23] M. S. Islam, J. Sultana, M. Faisal, M. R. Islam, A. Dinovitser, B. W. H. Ng, and D. Abbott, "Modified hexagonal photonic crystal fiber for terahertz applications," *Optical Materials*, vol. 79, pp. 336–339, May 2018.

[24] T. Yang, C. Ding, R. W. Ziolkowski, and Y. J. Guo, "Circular hole enz photonic crystal fibers exhibit high birefringence," *Optics. Expres*, vol. 26, pp. 17264-17278, June 2018.

[25] T. Yang, C. Ding, R. W. Ziolkowski, and Y. J. Guo, "Scalable THz photonic crystal fiber with partially-slotted core that exhibits improved birefringence and reduced loss," *Journal of Lightwave Technology*, vol. 36, pp. 3408-3417, August 2018.

[26] I. K. Yakasai, A. Rahman, P. E. Abas, and F. Begum, *Theoretical Assessment of a Porous Core Photonic Crystal Fiber for Terahertz Wave Propagation*, Artice in Press, 2018.

[27] K. Nielsen, H. K. Rasmussen, A. J. Adam, P. C. Planken, O. Bang, and P. U. Jepsen, "Bendable, low-loss topas fibers for the terahertz frequency range," *Optics Express*, vol. 17, pp. 8592-8601, May 2009.

[28] F. Begum and P. E. Abas, "Near infrared supercontinuum generation in silica based photonic crystal fiber," *Progress in Electromagnetic Research C*, vol. 89, pp. 149–159, January 2019.

[29] I. K. Yakasai, P. E. Abas, W. Caesarendra, and F. Begum, "Proposal for a quad-elliptical photonic crystal fiber for terahertz wave guidance and sensing chemical warfare liquids," *Multidisciplinary Digital Publishing Institute*, vol. 6, no. 3, pp. 78-93, July 2019.